Supplementary Information

Improving the performance of gliding arc plasma-catalytic dry reforming via a new post-plasma tubular catalyst bed

Wencong Xu[a,b,c*], Lukas C. Buelens[c], Vladimir V. Galvita[c], Annemie Bogaerts[b], Vera Meynen[a]

[a] Laboratory of Adsorption and Catalysis, Department of Chemistry, University of Antwerp (CDE), Universiteitsplein 1, B-2610 Wilrijk, Antwerp, Belgium

[b] Plasma Lab for Applications in Sustainability and Medicine-Antwerp, Department of Chemistry, University of Antwerp (CDE), Universiteitsplein 1, Wilrijk, B-2610, Belgium

[c] Laboratory for Chemical Technology, Department of Materials, Textiles and Chemical Engineering, Ghent University, Technologiepark 125, B-9052, Ghent, Belgium

*Corresponding author: wencong.xu@uantwerpen.be

Content of supplementary information

S1 Details for the characterizations of catalyst

X-ray diffraction (XRD) was performed using an X'Pert Pro X-ray generator. The incident beam went through a Soller slit with a width of 0.04° combined with a programmable divergence slit with an irradiated length of 10.0 mm. The diffracted beam system has an automatic anti-scatter slit (observed length: 10.0 mm and height 0.3 mm), after which there is another Soller slit with 0.04 radians. Behind the Soller slit, a graphite monochromator and a proportional detector were present. Samples were ground in an agate mortar, placed in a monocrystal holder and mounted on a sample stage, which is a spinner. The samples were spinning with a revolution time of one second. It was operated at 40 kV and 40 mA with CuK_α radiation in the 2θ scanning range of 5-70° with a step size of 0.04° and 4 s/step. The measurements were done under atmospheric conditions at room temperature.

The specific surface area was deduced from the isotherms recorded on a Quantachrome Quadrasorb SI automated gas adsorption system. Before analysis, all the samples were degassed at 80 °C (which is also the temperature for drying the samples) for 16 h under high vacuum condition. Multipoint BET was used to determine the apparent surface area.

Hydrogen-temperature programmed reduction (H_2-TPR) were conducted to collect the reduction data of the sample. The measurements were performed on a ChemStar TPX Chemisorption Analyzer from Anton Paar. Typically, 50 mg sample was pretreated at 350 °C for 1 h in 50 mL/min He. Subsequently, after cooling down to 50 °C, the sample was fully oxidized by 5% O_2/He gas at a flow rate of 50 mL/min. During the process, the temperature increased from 50 °C to 800 °C with a rate of 10 °C/min. A maximum temperature of 800 °C was chosen not to exceed the calcination temperature, preventing changes made to the materials during analysis. After the cooling of the sample down to 50 °C by He, the H_2-TPR procedure was conducted to 1000 °C with a rate of 10 °C/min while flowing 5% H_2/Ar at 50 mL/min.

Thermogravimetric (TG) analysis was performed on a 100 mg mixture of catalyst and α-Al_2O_3 after plasma or thermal catalytic DRM reaction to analyze the carbon deposition on the catalysts, using a Mettler Toledo TGA/SDTA851e thermal balance coupled with a Hiden HPR-20 R&D Mass Spectrometer (MS). Specifically, the sample was heated to 1000 ℃ under a flow of 80 mL/min O_2 with a heating rate of 10 ℃/min to determine the deposited carbon content. The MS signals for m/z

within the range of 2 to 100 were collected. In addition, Raman spectra (Xplora Plus, Horiba Scientific) were recorded to understand the crystal structure of the carbon collected after plasma reaction from the reactor tube or on the catalyst. The Raman spectra were measured at a laser excitation wavenumber of 532 nm (with filter value of 10%) in a spectral range of 100–3500 cm^{-1}.

S2 Tables

Table S1. Selectivity, yield, H_2/CO ratio and carbon balance results of DRM in thermal catalytic reaction.

Temperature (° C)	Selectivity (%)		Yield (%)		H_2/CO ratio	C balance
	CO	H_2	CO	H_2		
800	88	100	81	80	0.9	89
700	89	100	73	70	0.9	91
600	92	100	48	41	0.8	96
500	100	100	18	11	0.6	101
400	100	100	3	1	0.3	103

Table S2. Carbon balance for different plasma and plasma-catalytic DRM configurations. Gas composition: N_2:CH_4:CO_2 = 8:1:1 or 8:0.6:1, GHSV: 480 $L \cdot g^{-1}h^{-1}$.

Configurations	Carbon balance (%)	
	$CH_4/CO_2 = 1$	$CH_4/CO_2 = 0.6$
Plasma alone	92.9±0.7	98.7±0.8
T-bed-3 Ni/MO	96.2±1.6	99.7±1.6
N-bed Ni/MO	100.8±0.8	100.5±0.7
N-bed α-Al_2O_3	100.2±1.0	100.2±0.6

S3 Figures

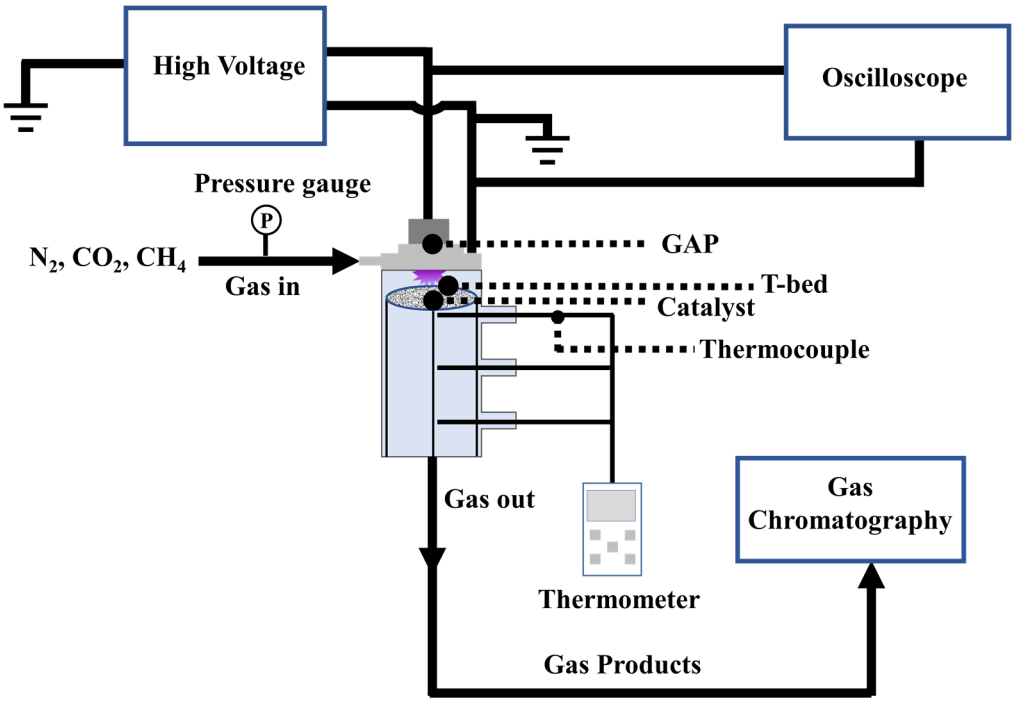

Fig. S1. Schematic diagram of the GAP DRM experimental setup.

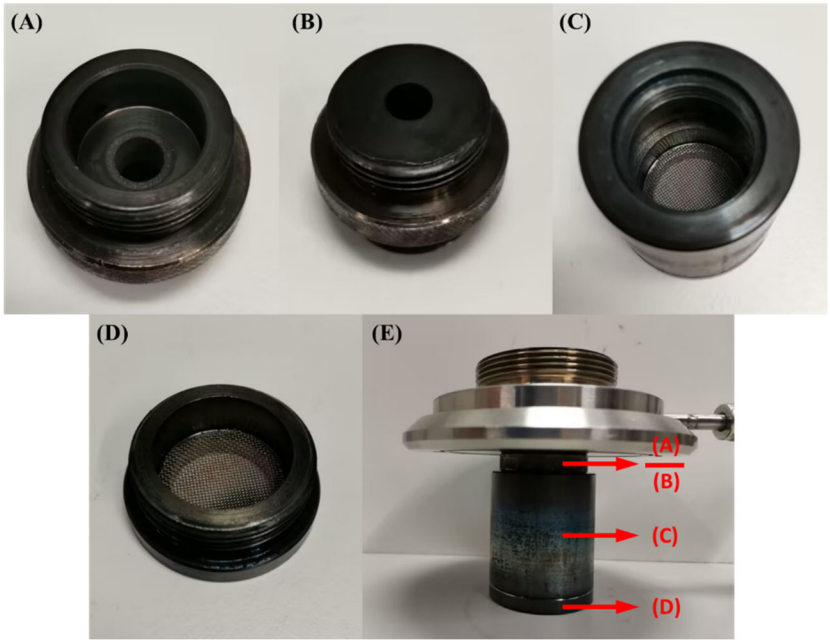

Fig. S2. Photographs of the N-bed. (A)&(B) the top and bottom sides of the connector. (C) tubular body of the N-bed. (D) bottom with metal mesh of the N-bed. (E) N-bed connection to the plasma device part.

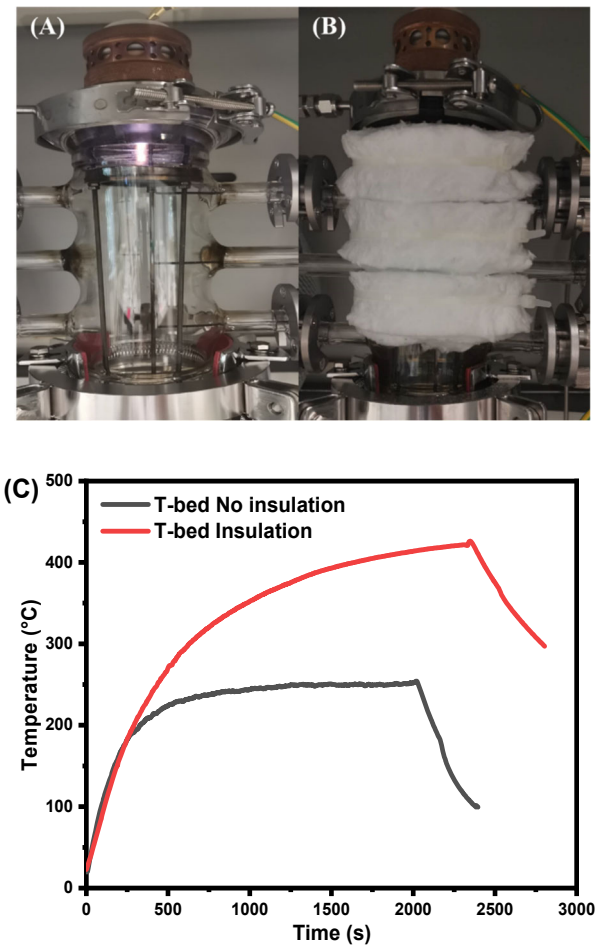

Fig. S3. Photographs of the GAP setup without (A) and with (B) insulation, and (C) temperature measured after the catalyst bed during the reaction. Gas composition: $N_2/CH_4/CO_2$ = 8/1/1, GHSV: 480 $L \cdot g_{cat}^{-1} \cdot h^{-1}$.

Fig. S4. Results of conversion and selectivity obtained in the T-bed configuration at a distance of 4 cm, with or without insulation in the GAP DRM system. Gas composition: N_2:CH_4:CO_2 = 8:1:1, GHSV: 480 $L \cdot g_{cat}^{-1} \cdot h^{-1}$.

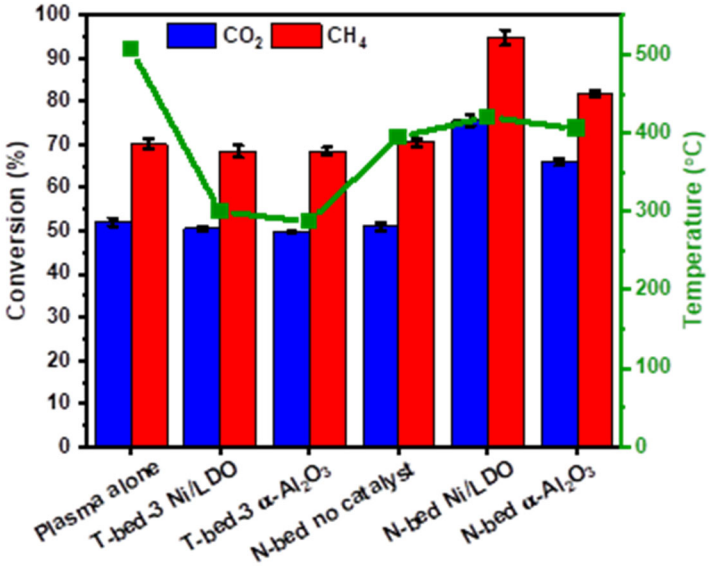

Fig. S5. Conversion (left y-axis) of CO_2 and CH_4 and temeprature (right y-axis) at 4.9 cm after 15 min plasma reaction in the GAP post-plasma-catalytic DRM at different conditions with a CH_4:CO_2 ratio of 0.6. Gas composition: N_2: 6.4 L/min, CH_4: 0.6 L/min, CO_2:1 L/min (CH_4/CO_2=0.6), GHSV: 480 $L \cdot g_{cat}^{-1} \cdot h^{-1}$.

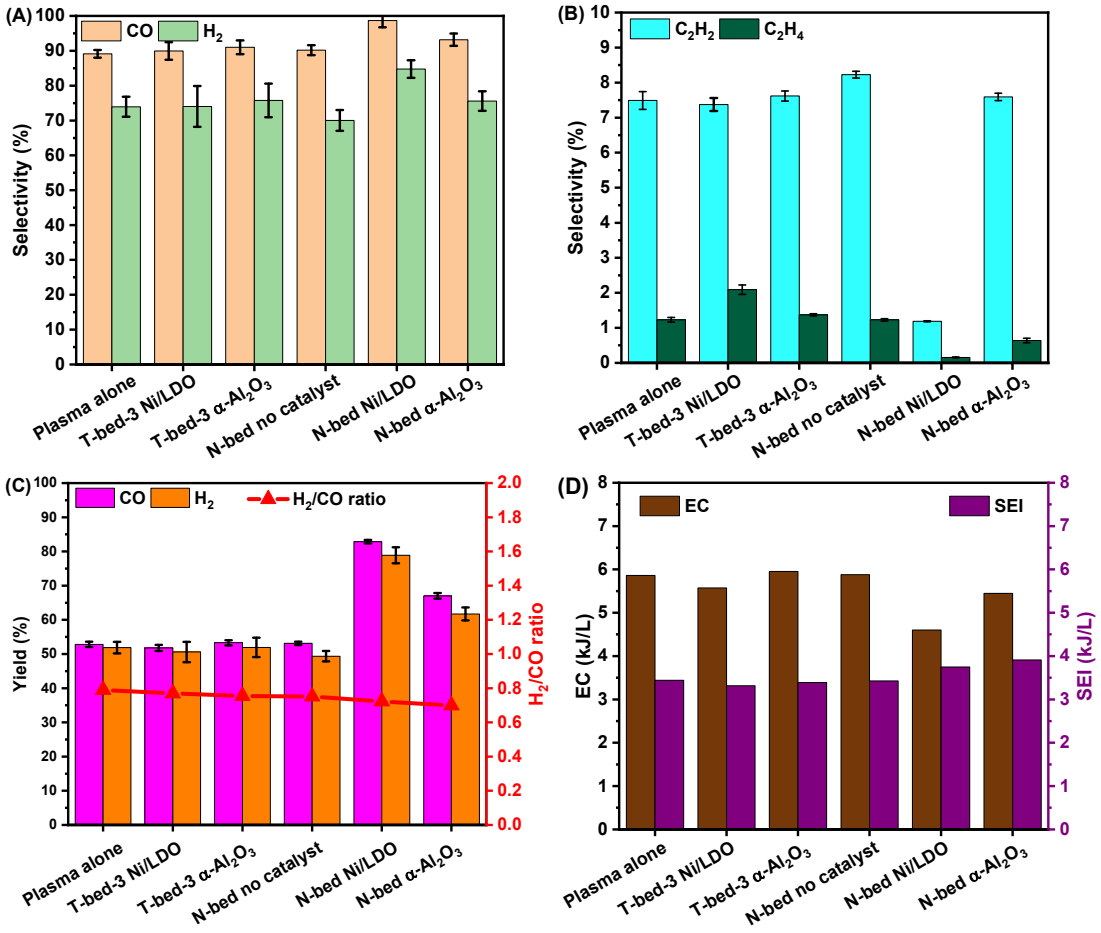

Fig. S6. Selectivity, yield, H_2/CO ratio, EC and SEI result for a CH_4/CO_2 ratio of 0.6 in the GAP PPC DRM reaction. (A) Selectivity of CO and H_2, (B) Selectivity of C_2H_2 and C_2H_4, (C) Yield of CO and H_2 and H_2/CO ratio, and (D) Energy cost (EC) of the conversion and specific energy input (SEI) into the system in different configurations. Gas composition: N_2: 6.4 L/min, CH_4: 0.6 L/min, CO_2:1 L/min (CH_4/CO_2=0.6), GHSV: 480 $L \cdot g_{cat}^{-1} \cdot h^{-1}$.

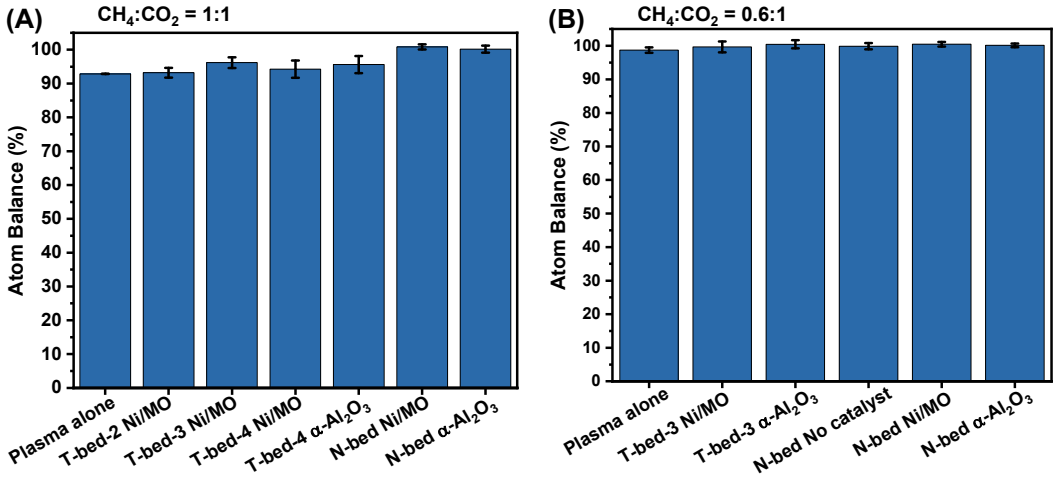

Fig. S7. Carbon balance in different cases. Gas composition: (A) N_2:CH_4:CO_2 = 8:1:1, (B) N_2:CH_4:CO_2 = 8:0.6:1, GHSV: 480 $L \cdot g_{cat}^{-1} \cdot h^{-1}$.

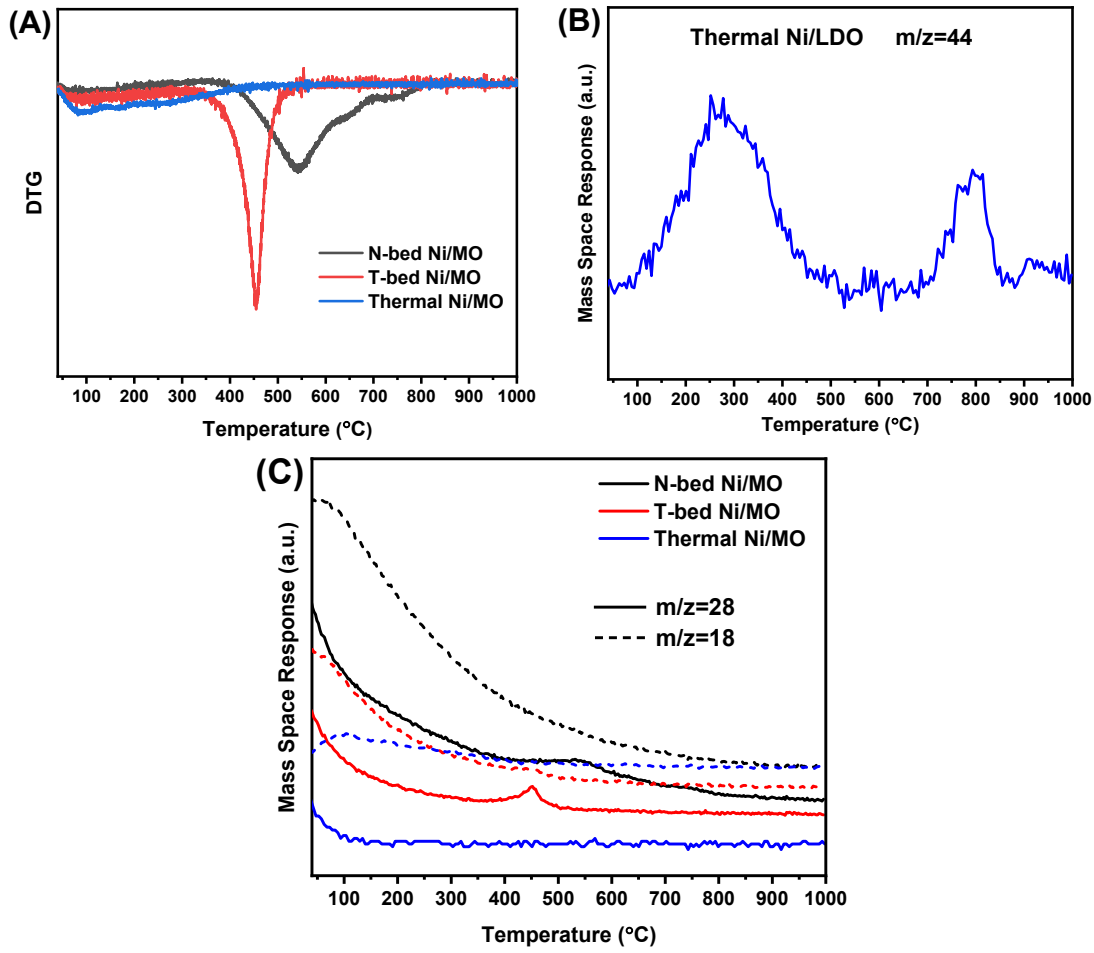

Fig. S8. (A) DTG of Ni/MO catalyst in different cases after reaction, (B) Enlarge figure of MS result with m/z=44 for thermal Ni/MO catalyst case, and (C) MS result (m/z=28 and 18) of Ni/MO catalyst in the different cases after reaction. Gas composition: N_2:CH_4:CO_2 = 8:1:1, GHSV: 480 $L \cdot g_{cat}^{-1} \cdot h^{-1}$.

S3 Equations for calculation of the performance metrics in plasma-based DRM

To calculate the performance metrics in case of $CO_2/CH_4/N_2$ DRM, the formulas were used as reported in the literature [1–3] (references listed at the end). Considering the gas expansion, the expansion factor can be determined by adding an internal standard gas to the outlet gas flow stream after the reactant gas has passed through the plasma. Internal standard gasses can in principle be N_2, He, or Ar. However, in our case, He is impossible as it is the carrier gas of the GC. Neither can Ar be used, as its peak overlaps with the one of O_2. For N_2, in principle, it is also not a suitable gas, because it is used in the mixture which passes through the GAP reactor. However, considering the conversion of N_2 in the GAP plasma DRM is barely converted (< 0.05%) [4,5], it is used in our case as the internal standard gas. Two correction factors α and β were defined via the following equations:

$$\beta = \frac{\mathrm{N}_{2,in}}{CO_{2,in} + CH_{4,in}} \quad \text{(S1)}$$

where $\mathrm{N}_{2,in}$, $CO_{2,in}$, and $CH_{4,in}$ were the gas flow rate of N_2, CO_2, and CH_4 in the feed gas, respectively.

The value of α is corrected by β with equation (S2):

$$\alpha = \frac{\mathrm{N}_{2,\mathrm{blank}}}{\mathrm{N}_{2,\mathrm{plasma}}}(1+\beta) - \beta \quad \text{(S2)}$$

Where $\mathrm{N}_{2,\mathrm{blank}}$ and $\mathrm{N}_{2,\mathrm{plasma}}$ represent the amount of N_2 measured before and after starting the plasma.

The concentrations were corrected with equation (S3):

$$\mathrm{C}_{\mathrm{i,out}} = \mathrm{C}_{\mathrm{i,out,m}}(1+\beta/\alpha) \quad \text{(S3)}$$

Where $\mathrm{C}_{\mathrm{i,out,m}}$ means the concentration of sample i, i.e., CH_4, CO_2, CO, and H_2, measured by the GC.

The absolute conversion of CO_2, $\mathrm{X}_{\mathrm{abs},\mathrm{CO}_2}$ and effective conversion of CO_2, $\mathrm{X}_{\mathrm{eff},\mathrm{CO}_2}$ were calculated with equation (S4) and equation (S5), respectively. $\mathrm{C}_{CO_{2,in}}$ was the concentration of CO_2 measured going through the GAP before the plasma was turned on. $\mathrm{C}_{CO_{2,out}}$ was the concentration of outlet gas.

$$X_{abs,CO_2}(\%) = \frac{C_{CO_{2,in}} - C_{CO_{2,out}}}{C_{CO_{2,in}}} \times 100\% \quad (S4)$$

$$X_{eff,CO_2}(\%) = X_{abs,CO_2}(\%) \cdot Fraction_{CO_2} \quad (S5)$$

where $Fraction_{CO_2}$ means the concentration of CO_2 in the inlet gas.

The absolute and effective conversions of CH_4 were defined as equation (S6) and equation (S7):

$$X_{abs,CH_4}(\%) = \frac{C_{CH_{4,in}} - C_{CH_{4,out}}}{C_{CH_{4,in}}} \times 100\% \quad (S6)$$

$$X_{eff,CH_4}(\%) = X_{abs,CH_4} \cdot Fraction_{CH_4} \quad (S7)$$

The C-based selectivity of CO and other chemicals including carbon atoms, the H-based selectivity of H_2, and the yield of CO, and H_2 were defined as equations from (S8) to (S12):

$$S_{H_2} = \frac{C_{H_{2,out}}}{2 \times (C_{CH_{4,in}} - C_{CH_{4,out}})} \times 100\% \quad (S8)$$

$$S_{CO} = \frac{C_{CO_{out}}}{(C_{CH_{4,in}} - C_{CH_{4,out}}) + (C_{CO_{2,in}} - C_{CH_{2,out}})} \times 100\% \quad (S9)$$

$$S_{C_xH_yO_z} = \frac{x \times C_{C_xH_yO_{z,out}}}{(C_{CH_{4,in}} - C_{CH_{4,out}}) + (C_{CO_{2,in}} - C_{CH_{2,out}})} \times 100\% \quad (S10)$$

$$Y_{CO} = \frac{Fraction_{CH_4} \times X_{abs,CH_4} + Fraction_{CO_2} \times X_{abs,CO_2}}{(C_{CH_{4,in}} - C_{CH_{4,out}}) + (C_{CO_{2,in}} - C_{CH_{2,out}})} \times S_{CO} \quad (S11)$$

$$Y_{H_2} = X_{abs,CH_4} \times S_{H_2} \quad (S12)$$

The specific energy input (SEI) and energy cost (EC) were defined as equation (S13) and equation (S14).

$$SEI(kJ/L) = \frac{\text{Plasma Power (kW)} \cdot 60\ (s/min)}{\text{Total gas flow rate (L/min)}} \quad (S13)$$

$$EC(kJ/L) = \frac{SEI\ (kJ/L)}{X_{eff,CO_2}} \quad (S14)$$

For the balance of C atoms in the products versus in the reactants, the equation was as followed:

$$Balance_C = \frac{\alpha \cdot (C_{CO_2(out)} + C_{CH_4(out)} + C_{CO(out)} + 2 \cdot C_{C_2(out)} + 3 \cdot C_{C_3(out)})}{C_{CO_2(in)} + C_{CH_4(in)}} \quad (S15)$$

References

[1] N. Pinhão, A. Moura, J. B. . Branco, J. Neves, Int. J. Hydrogen Energy **2016**, 41, 9245–9255.

[2] S. Van Alphen, J. Slaets, S. Ceulemans, M. Aghaei, R. Snyders, A. Bogaerts, J. CO2 Util. **2021**, 54, 101767.

[3] B. Wanten, S. Maerivoet, C. Vantomme, J. Slaets, G. Trenchev, A. Bogaerts, J. CO2 Util. **2022**, 56, 101869.

[4] E. Cleiren, S. Heijkers, M. Ramakers, A. Bogaerts, ChemSusChem **2017**, 10, 4025–4036.

[5] J. Slaets, M. Aghaei, S. Ceulemans, S. Van Alphen, A. Bogaerts, Green Chem. **2020**, 22, 1366–1377.